EuroIntervention
2024;20:e656-e668
published online e-edition May 2024
DOI: 10.4244/EIJ-D-23-00605

ORIGINAL RESEARCH

Impact of coronary calcium morphology on intravascular lithotripsy

Angela McInerney[1], MD; Alejandro Travieso[1], MD; Adrián Jerónimo Baza[1], MD; Fernando Alfonso[2], MD, PhD; David Del Val[2], MD, PhD; Enrico Cerrato[3,4], MD, PhD; Juan Garcia de Lara[5], MD, PhD; Eduardo Pinar[5], MD, PhD; Armando Perez de Prado[6], MD, PhD; Pilar Jimenez Quevedo[1], MD, PhD; Gabriela Tirado-Conte[1], MD; Luis Nombela-Franco[1], MD, PhD; Salvatore Brugaletta[7], MD, PhD; Pedro Cepas-Guillén[7], MD, PhD; Manel Sabaté[7], MD, PhD; Héctor Cubero Gallego[8], MD, PhD; Beatriz Vaquerizo[8], MD, PhD; Alfonso Jurado[9], MD, PhD; Ferdinando Varbella[3,4], MD; Marcelo Jimenez[10], MD, PhD; Artemio Garcia Escobar[9], MD; José María de la Torre[11], MD, PhD; Ignacio Amat Santos[12], MD, PhD; Victor Alfonso Jimenez Diaz[13], MD, PhD; Javier Escaned[1], MD, PhD; Nieves Gonzalo[1]*, MD, PhD

GUEST EDITOR: Franz-Josef Neumann, MD, PhD, FESC; *Department of Cardiology and Angiology II, University Heart Center Freiburg - Bad Krozingen, Bad Krozingen, Germany*

**Corresponding author: Hospital Clinico San Carlos, IdISSC, C/ Prof. Martin Lagos, s/n, 28040, Madrid, Spain. E-mail: nieves_gonzalo@yahoo.es*

The authors' affiliations can be found at the end of this article.

This paper also includes supplementary data published online at: https://eurointervention.pcronline.com/doi/10.4244/EIJ-D-23-00605

ABSTRACT

BACKGROUND: Coronary calcification negatively impacts optimal stenting. Intravascular lithotripsy (IVL) is a new calcium modification technique.

AIMS: We aimed to assess the impact of different calcium morphologies on IVL efficacy.

METHODS: This was a prospective, multicentre study (13 tertiary referral centres). Optical coherence tomography (OCT) was performed before and after IVL, and after stenting. OCT-defined calcium morphologies were concentric (mean calcium arc >180°) and eccentric (mean calcium arc ≤180°). The primary outcomes were angiographic success (residual stenosis <20%) and the presence of fracture by OCT in concentric versus eccentric lesions.

RESULTS: Ninety patients were included with a total of 95 lesions: 47 concentric and 48 eccentric. The median number of pulses was 60 (p=1.00). Following IVL, the presence of fracture was not statistically different between groups (79.0% vs 66.0% for concentric vs eccentric; p=0.165). The number of fractures/lesion (4.2±4.4 vs 2.3±2.8; p=0.018) and ≥3 fractures/lesion (57.1% vs 34.0%; p=0.029) were more common in concentric lesions. Angiographic success was numerically but not statistically higher in the concentric group (87.0% vs 76.6%; p=0.196). By OCT, no differences were noted in final minimum lumen area (5.9±2.2 mm^2 vs 6.2±2.1 mm^2; p=0.570), minimum stent area (5.9±2.2 mm^2 vs 6.25±2.4 mm^2; p=0.483), minimum stent expansion (80.9±16.7% vs 78.2±19.8%), or stent expansion at the maximum calcium site (100.6±24.2% vs 95.8±27.3%) (p>0.05 for all comparisons of concentric vs eccentric, respectively). Calcified nodules were found in 29.5% of lesions; these were predominantly non-eruptive (57%). At the nodule site, dissection was more common than fracture with stent expansion of 103.6±27.2%.

CONCLUSIONS: In this prospective, multicentre study, the effectiveness of IVL followed by stenting was not significantly affected by coronary calcium morphology.

KEYWORDS: calcified stenosis; drug-eluting stent; optical coherence tomography

SUBMITTED ON 27/07/2023 - REVISION RECEIVED ON 1st 14/10/2023 / 2nd 27/11/2023 / 3rd 19/12/2023 - ACCEPTED ON 20/12/2023

Coronary calcification continues to present a challenge in performing optimal percutaneous coronary intervention (PCI). Approximately 25% of patients presenting for PCI have a calcified lesion which is known to result in a higher incidence of major adverse cardiac events, particularly target lesion revascularisation (TLR) at midterm follow-up[1,2]. Many mechanisms have been put forward, including the difficulty in delivery of and mechanical damage to stents, as well as stent underexpansion. Stent underexpansion and, in particular, small minimum stent area (MSA) are known to be associated with stent failure[3,4]. The lack of compliance of calcified vessels is predominantly thought to account for poor expansion following stenting[5]. To address this problem, the use of plaque preparation techniques, whose aim is to improve vessel compliance prior to stenting, is recommended. One such technique is intravascular lithotripsy (IVL), a novel technique using a series of emitters encased within a balloon delivery system. Electrical pulses from the emitters are converted to acoustic energy waves within the balloon fluid and transmitted to the vessel wall[6]. When calcium is encountered, compression and decompression waves result in fracture, altering the rigidity of the atheromatous plaque and allowing expansion[6]. In this regard, the mechanism of action of IVL differs from those of high-pressure balloons or atherectomy techniques.

Initially, IVL was used predominantly in the context of severely calcified lesions defined by angiography. Data on the effectiveness of IVL in different calcified morphologies remain limited. Blachutzik et al used an angiographic definition of concentric and eccentric calcification and reported no differences in angiographic or clinical success[7]. However, angiography is known to be poorly sensitive for the detection of coronary calcium[8]. Conversely, intracoronary imaging with optical coherence tomography (OCT) has better sensitivity for calcium detection and provides unique insights on calcium location, distribution and pattern[8]. Recently, using an OCT definition, the effect of IVL on lesions containing nodules was reported[9]. However, reports on real-world experience of IVL and its effect on different calcium morphologies, as defined using intracoronary imaging, are limited. To address this void in knowledge, we performed a prospective, multicentre study with prespecified OCT assessment to determine the efficacy of IVL in different calcium morphologies.

Impact on daily practice

Coronary calcium is frequently encountered during percutaneous coronary intervention and negatively affects both the acute and long-term results of stenting. Calcium modification is recommended before stenting, but much debate exists regarding the most appropriate technique for concentric and eccentric calcium. In this prospective study, calcium morphology (concentric vs eccentric) did not significantly impact the effectiveness of intravascular lithotripsy, with no difference in final stent parameters as assessed by optical coherence tomography. These findings suggest that intravascular lithotripsy can be applied to patients with both concentric and eccentric calcium morphologies to optimise stent expansion.

Methods

STUDY POPULATION

This was an investigator-initiated, prospective, multicentre, single-arm study involving 13 tertiary care centres in Spain and Italy. Consecutive patients undergoing IVL for the treatment of calcified coronary artery disease were included. Patients were excluded if they required atherectomy techniques (rotational, orbital or laser) prior to IVL treatment or if they had chronic kidney disease with an estimated glomerular filtration rate <15 ml/min/1.73 m^2. All patients signed written informed consent, and the study was approved by the ethics committee at each participating centre. Follow-up for clinical events was also performed at the participating centres, and standard definitions for clinical events were used[10]. The study was registered at ClinicalTrials.gov: NCT04698902.

INTRAVASCULAR LITHOTRIPSY PROCEDURE

Centres were advised to select an IVL balloon based on vessel sizing by OCT. A 1:1 balloon-artery ratio was recommended. The number of pulses per cycle and total number of pulses delivered were at the discretion of the treating physician. Dilation after IVL was also at the discretion of the treating physician, while predilation was recommended only in the case of failure to advance an intracoronary imaging catheter.

OPTICAL COHERENCE TOMOGRAPHY PROCEDURE

OCT was mandatory and prespecified. It was performed using commercially available systems (Dragonfly OpStar [Abbott] and Lunawave [Terumo]) and was mandated prior to IVL treatment, immediately following IVL treatment and after final stenting and optimisation. Predilation with a small semicompliant balloon was permitted before IVL treatment to allow passage of the IVL or imaging catheter. All centres transferred both angiographic and OCT images to the coordinating centre for core lab analysis.

ANGIOGRAPHIC ANALYSIS

Quantitative coronary angiography (QCA) of procedural angiograms was performed in a core lab (Hospital Clínico San Carlos, Madrid, Spain) using the Caas Workstation software (Pie Medical Imaging). Lesion parameters were assessed by QCA at baseline, after IVL and after stenting. The examined parameters included percentage diameter stenosis (%DS),

Abbreviations

AKI	acute kidney injury	**eGFR**	estimated glomerular filtration rate	**OCT**	optical coherence tomography
BMI	body mass index	**IVL**	intravascular lithotripsy	**TLR**	target lesion revascularisation
BSA	body surface area	**MLA**	minimum lumen area		
CAD	coronary artery disease	**MSA**	minimum stent area		

lesion length, and calcium length. The acute gain by QCA was calculated as post-PCI minimum lumen diameter–pre-PCI minimum lumen diameter.

OPTICAL COHERENCE TOMOGAPHY ANALYSIS

OCT analysis was also performed in a core lab (Hospital Clínico San Carlos, Madrid, Spain) using dedicated software (AptiVue Offline Review Software [Abbott] or QIVUS [Medis Medical Imaging Systems] for OCTs performed using Lunawave). Cross-sectional OCT analysis was performed at 1 mm intervals along the entire lesion length. Standard OCT definitions were used[11]. The Fujino calcium score, which predicts stent underexpansion, was also calculated[12]. Calcium was defined as a signal-poor region with well-demarcated borders. The mean reference (proximal+distal/2) diameters and areas were used in all analyses. The mean calcium arc along the length of the lesion treated with IVL was calculated by summing the calcium arc at each 1 mm interval and dividing by the total length of the lesion in mm. Concentric calcium was defined as a mean calcium arc along the length of the lesion of >180 degrees. Eccentric calcium was a mean calcium arc along the length of the lesion of ≤180 degrees. Nodular calcium was defined as a calcific protrusion into the lumen and was further classified as eruptive (nodular protrusion into the lumen with an irregular surface and no overlying fibrous cap) or non-eruptive (nodular protrusion into the lumen with a smooth surface and a fibrous cap). A subanalysis of lesions containing nodules was performed to assess fracture and expansion following IVL in nodular calcium. Following IVL and stenting, nodules were defined as being deformed (compression of the nodule following stenting without significant luminal protrusion) or non-deformed (no/minimal compression of the nodule following stenting with persistent protrusion into the lumen).

The area stenosis was calculated as (mean reference lumen area–minimum lumen area [MLA])/mean reference lumen area). Stent expansion was calculated as (MSA/mean reference lumen area)*100. The mean stent expansion and stent expansion at the maximum calcium site were calculated in the same way. The asymmetry index was calculated as 1–(minimum lumen diameter of the entire segment/maximum lumen diameter of the entire segment), with a value ≥0.3 considered asymmetric. The eccentricity index was calculated as the minimum lumen diameter/maximum lumen diameter from the same cross-section, with a value ≤0.7 considered eccentric[13].

STUDY ENDPOINTS

The primary angiographic endpoint was angiographic success, defined as a residual stenosis following IVL and stenting of <20% in concentric versus eccentric calcification. The primary OCT endpoint was the number of fractures in concentric versus eccentric calcification. Secondary outcomes included the length and depth of fracture, stent expansion, stent malapposition, and MSA in concentric versus eccentric calcium.

STATISTICAL METHODS

Categorical variables were expressed as number and percentage (%), while continuous variables were expressed as mean and standard deviation (SD) or median and interquartile range (IQR) depending on the distribution. Normality was assessed using the Shapiro-Wilk test. Categorical variables were compared using the χ^2 or Fisher's exact test, and differences in continuous variables were compared using a 2-sided t-test or the Wilcoxon rank-sum test. Freedom from all-cause mortality and TLR at 12 months were calculated using the Kaplan-Meier method. All data were analysed using STATA 15.1 (StataCorp).

Results

Ninety-six patients (102 lesions) were included from 13 centres. After assessment, 6 patients (7 lesions) were excluded because of poor OCT quality, resulting in a cohort of 90 patients with a total of 95 lesions **(Supplementary Figure 1)**. By OCT, 47 lesions had predominantly concentric calcification, while 48 had predominantly eccentric calcification **(Central illustration)**. Patient demographics are shown in **Table 1**. The mean age was 72.5±9.1 years with a male predominance (73.3%). Most patients had chronic coronary syndromes. The left anterior descending artery (LAD) was the most commonly treated vessel.

There were no differences in procedural aspects between concentric and eccentric lesions **(Table 2)**. A high proportion of predilation was performed (62.2% vs 72.9%; p=0.270 for concentric vs eccentric, respectively). One IVL catheter per lesion was used in most cases, with the maximum IVL balloon diameter being 3 mm in both groups (p=1.00). The mean IVL balloon-artery ratio was ~1.2 by QCA and OCT across both groups (p>0.05). The median number of IVL pulses delivered was 60, without differences across the groups (p=1.00). Most lesions were stented using 1 stent and >90% were postdilated across both groups. One distal wire perforation occurred, which was managed conservatively. No perforations occurred during or after IVL therapy. Slow flow was seen in 2 patients, although neither case was related to the IVL therapy (1 before IVL therapy and 1 after stenting). Distal edge dissection that required further stenting occurred in 3 lesions. Transient side branch loss occurred in 1 patient after stenting using a provisional approach. There were no in-hospital deaths following IVL therapy.

LESION ASSESSMENT BY QUANTITATIVE CORONARY ANGIOGRAPHY

Table 3 and **Figure 1** show QCA parameters before IVL, after IVL and after stenting. A sequential decrease was seen in the %DS from baseline to after IVL and after stenting for both calcium morphologies. No difference in final %DS was found between groups (12.2±11.1% vs 12.5±10.0% for concentric vs eccentric calcium, respectively; p=0.894). Acute luminal gain was not different between groups (1.27±0.45 mm vs 1.25±0.51 mm; p=0.820). The primary outcome of angiographic success by QCA was numerically higher in the concentric group, but this was not statistically significant (87.0% vs 76.6%; p=0.196). Thrombolysis in Myocardial Infarction (TIMI) III flow was achieved in 98% of lesions without between-group differences.

LESION ASSESSMENT BY OPTICAL COHERENCE TOMOGRAPHY

OCT demonstrated a significant calcium burden across both groups **(Table 4)**. As expected, based on the

EuroIntervention Central Illustration

Overview of the important study findings.

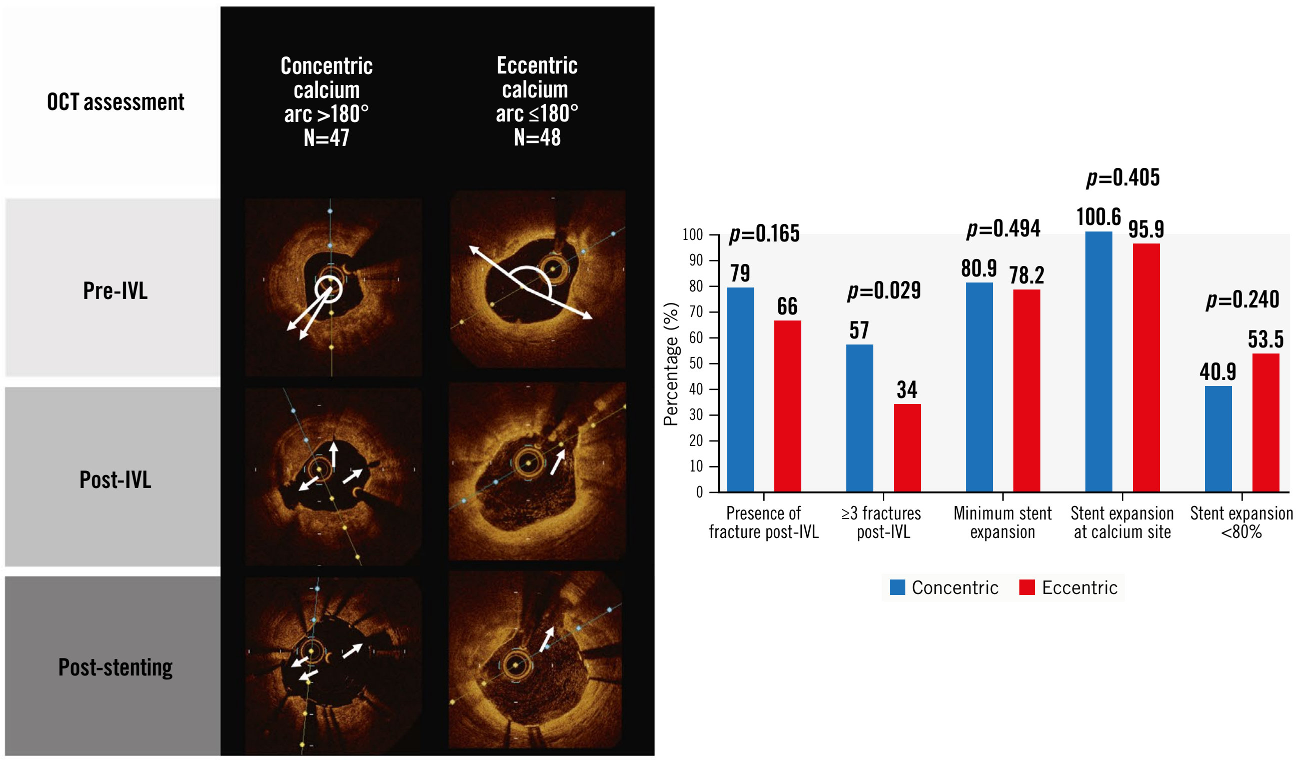

Angela McInerney *et al.* • *EuroIntervention* 2024;20:e656-e668 • DOI: 10.4244/EIJ-D-23-00605

The OCT images (A) depict typical findings in concentric and eccentric lesions, with white arrows highlighting the fracture within the calcium. B) The chart depicts the main results after IVL and stenting in concentric and eccentric lesions.
IVL: intravascular lithotripsy; OCT: optical coherence tomography

definitions used, concentric lesions had a larger mean calcium arc (229.9±47.2 degrees vs 145.8±27.9 degrees), maximum calcium arc (339.9±31.2 degrees vs 269.1±67.6 degrees) and calcium volume index (4,424±2,492 vs 2,739±1,720) than eccentric lesions (p<0.05 for all comparisons). Baseline percentage area stenosis (69.9±12.7% vs 64.8±14.6%; p=0.079) and MLA (1.78±0.74 mm² vs 1.99±0.68 mm²; p=0.151) were not different across groups, but concentric lesions tended towards greater percentage stenosis and a smaller MLA. The OCT calcium score (as defined by Fujino et al[12]) was 4 in most patients.

Following IVL, visible calcium fracture by OCT was numerically more common in concentric lesions, but without statistical significance (79% vs 66%; p=0.165). All other fracture parameters were greater in concentric than in eccentric lesions, including the total number of fractures per lesion (4.2±4.4 vs 2.3±2.8; p=0.018), the presence of 3 fractures per lesion (57.1% vs 34.0%; p=0.029), fracture width (0.62±0.29 mm vs 0.42±0.27 mm; p=0.005), fracture depth (0.92±0.35 mm vs 0.68±0.35 mm; p=0.008) and fracture arc (37.2±23.9 degrees vs 24.5±14.6 degrees; p=0.014) **(Central illustration, Figure 2)**. Dissection was common and occurred in three-quarters of lesions after IVL. Typical OCT findings in concentric and eccentric calcium are presented in the **Central illustration**.

A sequential increase in MLA across both groups following IVL and stenting was seen without differences in final in-stent MLA (5.9±2.2 mm² vs 6.2±2.1 mm² for concentric vs eccentric, respectively; p=0.570) **(Figure 3)**. Similarly, there were no differences in MSA between groups (5.9±2.2 mm² vs 6.25±2.4 mm² for concentric vs eccentric, respectively; p=0.483) **(Figure 2)**. Stent parameters such as minimum stent expansion (80.9±16.7% vs 78.2±19.8%) and expansion at maximum calcium site (100.6±24.2% vs 95.9±27.3%) were not different between groups (p>0.05 for all comparisons) **(Central illustration)**. Stent symmetry and eccentricity indices improved following stenting and were not different between groups. Significant malapposition (>0.4 mm) was more common in eccentric lesions.

NODULAR CALCIFICATION

Calcified nodules were present in 28 lesions (29.5%) **(Table 5)**. Almost half the nodules were within lesions in the LAD; however, as a proportion, nodules were more frequent in the right coronary (9 of 18) and left circumflex (4 of 10) arteries. The presence of a calcified nodule within a lesion was associated with an overall high burden of calcium, with the maximum calcium arc being 282 degrees and calcium thickness being 1.27 mm.

Table 1. Baseline demographics of patients undergoing IVL treatment.

	N=90
Age, years	72.5±9.1
Female sex	24 (26.7)
Body mass index, kg/m^2	28.1±4.1
Diabetes mellitus	41 (45.5)
Insulin use	12 (29.3)
Hypertension	69 (76.7)
Hyperlipidaemia	71 (78.9)
Smoking	36 (40.0)
Baseline eGFR, ml/min/1.73 m^2	78.5±19.1
eGFR <60 ml/min/1.73 m^2	14 (15.7)
Coronary artery disease	38 (42.2)
Previous MI	22 (24.4)
Previous PCI	26 (28.9)
Prior CABG	7 (7.8)
Atrial fibrillation	11 (12.2)
Previous permanent pacemaker	4 (4.4)
COPD	8 (8.9)
Previous cerebrovascular accident/TIA	5 (5.6)
Peripheral vascular disease	9 (10.0)
Baseline haemoglobin, g/dl	13.0±1.6
LVEF, %	54.6±9.6
Indication for PCI	
Stable angina/silent ischaemia	56 (62.2)
Acute coronary syndrome: unstable angina, STEMI, NSTEMI	34 (37.8)
Procedural aspects	
Vascular access	
Radial artery	74 (82.2)
Femoral artery	16 (17.8)
Contrast volume, ml	222.0±86.9
Procedure time, min	88 [63-170]
Acute kidney injury after procedure – all stage 1*	5 (6.8)
Vascular access complications	4 (5.1)
Length of hospital stay, days	2 [1-4]
In-hospital deaths	0 (0)
Medications on discharge	
Aspirin	88 (97.8)
Second antiplatelet	84 (93.3)
Anticoagulant	11 (12.8)
Statin	80 (89.9)

Data are presented as mean±SD, n (%) or median [IQR]. *Data available for 74 patients. CABG: coronary artery bypass grafting; COPD: chronic obstructive pulmonary disease; eGFR: estimated glomerular filtration rate; IQR: interquartile range; IVL: intravascular lithotripsy; LVEF: left ventricular ejection fraction; MI: myocardial infarction; NSTEMI: non-ST-segment elevation myocardial infarction; PCI: percutaneous coronary intervention; SD: standard deviation; STEMI: ST-segment elevation myocardial infarction; TIA: transient ischaemic attack

Nodule morphology was predominantly non-eruptive (57%) with the mean nodule arc spanning two quadrants (109.2±34 degrees). In 5 lesions, the nodule was at the MLA site. A progressive reduction in %DS with a corresponding increase in area at the nodule site was seen by OCT following IVL and stenting. At the site of the calcified nodule, dissection was common, while calcium fracture was less frequently seen. However, within lesions containing nodules, fracture in other calcified areas with nodules was common and seen in >70%. Stent expansion at the nodule site was 103.6±27.2%. Following stenting, only 40.7% of nodules were fully deformed and no longer protruding into the lumen. Malapposition at the nodule site was frequent, and malapposition >0.4 mm within the lesion containing a nodule was found in >70%. **Figure 4** depicts eruptive and non-eruptive nodules by OCT as well as the appearance of deformed and non-deformed nodules after stenting.

CLINICAL FOLLOW-UP

The median follow-up was 362 days (IQR 238-498). No in-hospital deaths occurred. Freedom from all-cause mortality at 12 months was 96% **(Supplementary Figure 2)**. Three patients died during this time: 2 of non-cardiovascular causes and 1 of sudden cardiac death. Freedom from TLR was 96% **(Supplementary Figure 3)**. Four lesions required revascularisation, with the median time to TLR being 225 days (IQR 33-283). Two of these lesions presented as acute coronary syndromes with one being a definite stent thrombosis at 6 days after IVL.

Discussion

This prospective, multicentre study evaluated the effect of IVL on different calcium patterns. The main findings are as follows: 1) concentric and eccentric calcification were equally common in the present population; 2) while IVL results in calcium fracture in both concentric and eccentric calcification, IVL in concentric lesions results in a greater number of fractures, with wider, and deeper fractures; 3) despite greater fracture parameters in concentric calcium, there were no differences in final %DS by QCA between calcium morphologies; 4) OCT analysis confirmed that there were no differences in main stenting parameters including MSA, stent expansion and expansion at maximum calcium site, between concentric and eccentric calcium; 5) calcified nodules were found in 29.5% of lesions, and following IVL, dissection was more frequent than fracture at the nodule site; however, the mean stent expansion at the nodule site was >100%.

Calcified coronary artery disease is a frequent finding in the catheterisation lab and is not only a marker of lesion complexity but is also a marker of poor outcomes, both immediately and at longer term follow-up[1]. While a number of tools are available to treat coronary calcification, severe calcification often requires atherectomy techniques which have reported periprocedural complication rates of 2-4%[14-17]. Similar periprocedural complications have been reported with the use of modified and super-high pressure balloons[18,19]. IVL offers a different mechanism of action in terms of calcium modification and utilises acoustic waves generated from emitters encased within a balloon delivery system[6]. The safety and efficacy of IVL has been shown in the Disrupt CAD series of studies, and a pooled analysis of these studies has shown low complication rates (perforation

Table 2. Procedural aspects.

Procedural aspects per lesion	Overall population N=95	Concentric N=47	Eccentric N=48	*p*-value
Coronary artery treated				**0.381**
Left main stem	6 (6.3)	1 (2.1)	5 (10.4)	
Left anterior descending	61 (64.2)	31 (66.0)	30 (62.5)	
Left circumflex	10 (10.5)	6 (12.8)	4 (8.3)	
Right coronary	18 (18.9)	9 (19.2)	9 (18.7)	
Plaque modification pre-IVL				
Balloon predilation	63 (67.7)	28 (62.2)	35 (72.9)	0.270
Compliant balloon	49 (77.8)	23 (82)	26 (76.5)	0.787
Non-compliant balloon	16 (25.4)	7 (25)	9 (25.7)	0.541
Cutting/scoring balloon	14 (22.6)	7 (25)	7 (20.6)	0.506
Maximum diameter of predilation balloon, mm	2.5 [2.0-2.5]	2.25 [2.0-2.5]	2.5 [2.0-2.5]	<0.001
IVL characteristics				
Number of IVL balloons used per vessel				
1 IVL balloon	83 (88.3)	40 (87.0)	43 (89.6)	0.692
≥2 IVL balloons	11 (11.7)	6 (13.0)	5 (10.4)	0.511
Maximum diameter of IVL balloon used, mm	3.0 [2.5-3.5]	3.0 [2.5-3.5]	3.0 [3.0-3.5]	1.00
Balloon-artery ratio QCA	1.20±0.22	1.18±0.18	1.18±0.25	0.989
Balloon-artery ratio OCT	1.23±0.24	1.26±0.25	1.23±0.23	0.576
Number of pulses administered per vessel	60 [40-80]	60 [40-80]	55 [40-80]	1.00
Plaque modification post-IVL				
Balloon post-dilation	23 (24.5)	13 (28.3)	10 (20.8)	0.402
Balloon angioplasty (compliant)	3 (11.1)	2 (13.3)	1 (8.3)	0.681
Balloon angioplasty (non-compliant)	20 (86.9)	13 (86.7)	7 (58.3)	0.095
Cutting/scoring balloon	6 (22.2)	3 (20.0)	3 (25.0)	0.476
Maximum diameter of balloon after IVL, mm	3 [3.0-3.5]	3.25 [3.0-3.5]	3 [3.0-3.5]	1.00
PCI characteristics				
Number of stents per vessel	1 [1-1]	1 [1-1]	1 [1-1]	1.00
Total stented length, mm	26 [18-38]	26 [18-40]	26 [21-33.5]	1.00
Mean stent diameter, mm	3.0 [2.75-3.5]	3.0 [2.75-3.5]	3.0 [2.75-3.5]	1.00
Post-dilation	86 (92.5)	43 (93.5)	43 (91.5)	0.716
Maximum diameter of post-dilation balloon, mm	3.5 [3.0-3.5]	3.5 [3.0-3.5]	3.5 [3.0-3.5]	1.00

Data are presented as n (%), median [IQR] or mean±SD. IQR: interquartile range; IVL: intravascular lithotripsy; OCT: optical coherence tomography; PCI: percutaneous coronary intervention; QCA: quantitative coronary angiography; SD: standard deviation

rate 0.2%)[20]. Small retrospective studies have also demonstrated IVL to be safe[21].

Studies outside the Disrupt CAD series are, however, limited. Additionally, initial reports for the use of IVL shed doubt on its ability to fracture eccentric calcium. Our study represents a large, real-world cohort of patients with prespecified OCT assessment in both eccentric and concentric calcification and reports on both the safety and efficacy of this technique. Our population reflects those reported in other calcium modification studies, incorporating a predominantly male cohort with multiple cardiovascular risk factors[15,19,20]. Additionally, in keeping with other studies, rates of pre- and post-dilation were high[15]. Reassuringly, despite the mandatory use of three runs of OCT, contrast volumes were in line with previous studies[15,22].

Angiographic assessment showed no significant differences between concentric and eccentric lesions. A sequential decrease in %DS with a corresponding increase in MLA was found in both groups, without differences in the final %DS. Furthermore, a residual %DS <30% was seen in >95% of patients, which is consistent with previous IVL studies[20].

Similar to previous studies, the presence of calcium fracture was common across both groups, with concentric lesions having higher numbers of fractures, as well as deeper and wider fractures. A larger calcium arc has previously been associated with increased fracture following IVL, a finding that is reflected in our study given the greater number of fractures seen in concentric lesions[23]. Calcium fracture is widely considered to be necessary to alter vessel compliance and allow stent expansion, and this has been noted in other studies examining calcium modification techniques[24,25]. Stent expansion tended to be higher in the concentric group, with a greater proportion of lesions having a minimum stent

Table 3. Quantitative coronary angiography assessment of lesions pre-IVL, post-IVL, and post-stenting.

Procedural aspects – QCA data	Overall population N=95	Concentric N=47	Eccentric N=48	*p*-value
Angiographic characteristics				
Pre-IVL				
Lesion length by QCA, mm	20.4±9.7	21.5±10.9	19.3±8.4	0.270
Percentage stenosis by QCA, %	58.2±2.3	58.3±11.8	58.1±12.8	0.943
Minimum diameter by QCA, mm	1.14±0.38	1.14±0.33	1.15±0.43	0.921
Reference diameter, mm	2.7±0.58	2.72±0.61	2.69±0.56	0.797
Type B2/C lesion	89 (93.7)	44 (93.6)	45 (93.7)	1.00
Post-IVL				
Percentage stenosis by QCA, %	34.9±15.8	36.2±16.2	33.6±15.4	0.446
Minimum diameter by QCA, mm	1.63±0.43	1.61±0.42	1.66±0.44	0.592
Acute diameter gain, mm	0.31±0.67	0.29±0.62	0.34±0.72	0.712
Post-stenting and optimisation (in stent)*				
Percentage stenosis by QCA, %	12.4±10.5	12.24±11.1	12.53±10	0.894
Minimum diameter by QCA, mm	2.41±0.44	2.41±0.45	2.41±0.43	0.894
Acute luminal gain by QCA, mm	1.26±0.48	1.27±0.46	1.26±0.47	0.904
Final percentage stenosis <50%	92 (98.9)	45 (97.8)	47 (100)	0.545
Final percentage stenosis <30%	89 (95.7)	44 (95.7)	45 (95.7)	0.982
Final percentage stenosis <20%	76 (82.0)	40 (87.0)	36 (76.6)	0.196
TIMI III flow	90 (97.83)	42 (95.5)	48 (100)	0.135
Post-stenting and optimisation (in segment)				
Percentage stenosis by QCA, %	15.7±12.6	17.68±12.9	13.9±12.2	0.156
Minimum diameter by QCA, mm	2.05±0.48	2.01±0.45	2.08±0.50	0.503
Acute luminal gain by QCA, mm	0.9±0.52	0.88±0.51	0.91±0.54	0.767

Data are presented as mean±SD or n (%). *Data are available for 93 lesions. IVL: intravascular lithotripsy; QCA: quantitative coronary angiography; SD: standard deviation; TIMI: Thrombolysis in Myocardial Infarction

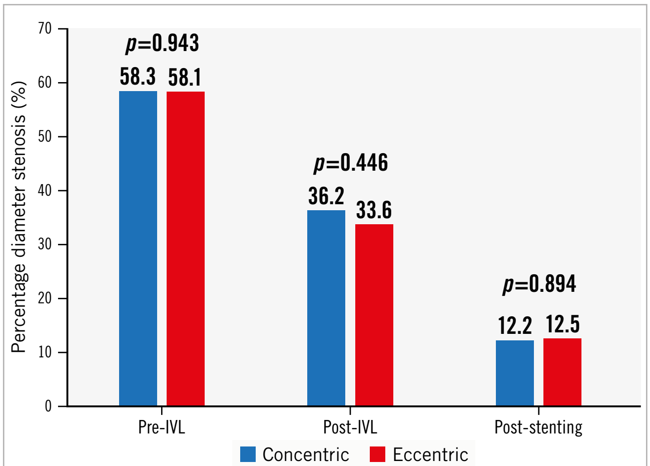

Figure 1. *Changes in percentage diameter stenosis by quantitative coronary angiography from baseline to after IVL, and after stenting (in stent). IVL: intravascular lithotripsy*

expansion >80%, which may have been related to the greater number of fractures in this group. However, overall, a high proportion of patients had stent expansion <80% (~50% of the entire cohort). Achieving optimum stent expansion in calcified lesions is difficult and excessive dilation may run the risk of perforation. In the PREPARE-CALC OCT substudy, which compared rotational atherectomy to modified balloons for calcified lesions, the minimum stent expansion across both groups was 73%, with >60% having expansion <80%[25]. Similar expansion was noted in the ISAR-CALC study, which compared super-high pressure balloons to modified balloons in calcified lesions (72% vs 68% for super-high pressure and modified balloons, respectively)[18]. Regarding IVL, OCT substudies of Disrupt CAD II and III found a minimum expansion of 77.6±20.5% and 78.4±25.8%, respectively[26,27], which overall aligns with our study, and is marginally better in comparison to the aforementioned studies using other techniques. Whether this small incremental increase in stent expansion with IVL translates to better longer-term outcomes versus other therapies remains to be elucidated.

Nodular calcium represents a morphology that is difficult to treat and is associated with stent recoil and device failure[28,29]. In our study, ~30% of lesions included a calcified nodule with a high proportion in the right coronary and left circumflex arteries, consistent with previous intracoronary imaging and post-mortem studies[9,30,31]. Following IVL therapy, fracture within a lesion containing a calcified nodule was common (70%); however, fracture within a nodule itself was uncommon

Table 4. Optical coherence tomography lesion assessment pre-IVL, post-IVL, and post-stenting.

Procedural aspects – OCT data	Overall population N=95	Concentric N=47	Eccentric N=48	*p*-value
Pre-IVL				
Lesion length, mm	23.7±10.7	24.0±11.7	23.5±9.6	0.852
Mean reference lumen area*, mm^2	6.4±2.6	6.58±3.0	6.23±2.1	0.531
Mean reference lumen diameter$, mm	2.79±0.58	2.81±0.66	2.77±0.50	0.740
Distal reference diameter, mm	2.56±0.67	2.58±0.80	2.52±0.55	0.741
Minimum lumen area, mm^2	1.88±0.71	1.78±0.74	1.99±0.68	0.151
Mean diameter at MLA, mm	1.51±0.30	1.46±0.29	1.55±0.31	0.154
Minimum diameter at MLA, mm	1.22±0.29	1.23±0.28	1.20±0.30	0.746
Percentage area stenosis, %	67.4±1.65	69.9±12.7	64.8±14.6	0.079
Percentage diameter stenosis, %	57.5±11.65	57.3±11.9	57.7±11.5	0.860
Asymmetry index**	0.69±0.1	0.69±0.1	0.69±0.1	0.775
Asymmetry index >0.3**	90 (100)	46 (100)	44 (100)	1.00
Eccentricity index**	0.49±0.1	0.52±0.1	0.47±0.1	0.034
Eccentricity index <0.7**	89 (98.8)	46 (100)	43 (97.7)	1.00
Extent of calcification				
Maximum calcium arc, degrees	304.5±62.2	339.9±31.2	269.1±67.6	<0.001
Lumen area at maximum calcium site, mm^2	3.13±1.58	2.77±1.49	3.50±1.61	0.030
Calcium thickness at maximum calcium site, mm	0.88±0.29	0.83±0.27	0.95±0.30	0.096
Mean calcium arc, degrees	188.3±57.3	229.9±47.2	145.79±27.9	<0.001
Calcium arc at MLA, degrees	259.6±95.3	303.8±76.6	215.4±92.3	<0.001
Calcium thickness at MLA, mm	0.85±0.33	0.87±0.32	0.82±0.36	0.604
Maximum calcium thickness, mm	1.13±0.25	1.1±0.26	1.18±0.24	0.075
Calcium length, mm	18.9±9.5	18.9±9.1	18.9±9.9	0.989
Calcium volume index	3,610±2,303	4,424±2,492	2,739±1,720	<0.001
Fujino OCT calcium score=4[12#]	86 (90.5)	45 (95.7)	41 (85.4)	0.091
Post-IVL				
Percentage area stenosis, %	43.5±15.1	43.5±16.3	43.5±14.0	1.00
Percentage diameter stenosis, %	40.2±13.4	38.9±12.6	41.4±14.1	0.384
Minimum lumen area, mm^2	3.6±1.14	3.6±1.2	3.6±1.1	0.860
Minimum diameter at MLA, mm	1.70±0.38	1.70±0.34	1.64±0.41	0.362
Mean diameter at MLA, mm	2.1±0.34	2.1±0.34	2.1±0.35	0.799
Post-IVL: calcium fracture characteristics	**n=89**	**n=89**	**n=89**	**n=89**
Presence of calcium fractures	65 (72.2)	34 (79)	31 (65.96)	0.165
≥3 visible fractures	40 (45)	24 (57.1)	16 (34.0)	0.029
Total number of fractures per lesion	3.18±3.7	4.2±4.4	2.3±2.8	0.018
Fracture width, mm	0.52±0.30	0.62±0.29	0.42±0.27	0.005
Fracture depth, mm	0.80±0.37	0.92±0.35	0.68±0.35	0.008
Length of fracture, mm	3.42±2.60	3.7±3.16	3.10±1.85	0.360
Fracture arc, degrees	31.25±20.95	37.2±23.9	24.5±14.6	0.014
Max no. of fractures per quadrant	1.12±0.63	1.29±0.62	0.97±0.61	0.035
No. of quadrants with fracture	2.1±1.3	2.6±1.1	1.7±1.2	0.002
Presence of dissections	64 (74.4)	31 (73.8)	33 (75.0)	0.899
Dissection depth, mm	0.42±0.17	0.44±0.18	0.40±0.15	0.444
Dissection arc, degrees	73.9±38.3	76.0±36.7	72.26±40.1	0.634
Dissection length, mm	2.85±2.18	2.56±1.37	3.10±2.65	0.577
Minimum calcium arc where fracture is seen, degrees	223.4±99.7	248.44±95.95	194.00±98.55	0.098
No. of fractures at max calcium site	1.02±1.1	1.14±1.1	0.90±1.1	0.308

Table 4. Optical coherence tomography lesion assessment pre-IVL, post-IVL, and post-stenting (cont'd).

Procedural aspects – OCT data	Overall population N=95	Concentric N=47	Eccentric N=48	*p*-value
Max no. of fractures per single frame	1.28±1.20	1.50±1.20	1.10±1.20	0.112
Calcium arc at max no. of fractures, degrees	271.4±106.4	293.5±97.6	248.4±112.1	0.132
Post-stenting (in stent)				
Minimum lumen area, mm^2	6.06±2.12	5.90±2.20	6.20±2.10	0.570
Minimum stent area, mm^2	6.08±2.26	5.90±2.18	6.25±2.40	0.483
Mean stent area, mm^2	7.94±2.55	7.70±2.60	8.14±2.50	0.455
Stent area at MLA, mm^2	6.98±2.10	6.97±2.10	7.00±2.14	0.939
Mean reference area, mm^2	7.93±3.19	7.62±3.24	8.23±3.15	0.373
Minimum stent expansion, %	79.6±18.25	80.9±16.67	78.2±19.77	0.494
Stent expansion <80%	47 (49.5)	18 (40.9)	24 (53.5)	0.240
Mean stent expansion, %	105.28±19.6	107.7±18.1	102.9±20.9	0.265
Stent area at max calcium site, mm^2	7.31±2.12	7.10±2.15	7.53±2.10	0.372
Stent expansion at maximum calcium site, %	98.3±25.6	100.6±24.2	95.9±27.3	0.405
Stent symmetry index	0.41±0.10	0.40±0.10	0.42±0.10	0.434
Stent symmetry index >0.3	80 (88.9)	40 (86.9)	40 (90.9)	0.551
Eccentricity index	0.67±0.09	0.68±0.10	0.67±0.08	0.644
Eccentricity index <0.7	53 (60.9)	27 (61.4)	26 (60.5)	0.932
Post-stenting (in segment)				
Minimum lumen area, mm^2	4.87±2.26	4.92±2.50	4.81±2.00	0.821
Malapposition				
Presence of malapposed struts	58 (65.2)	30 (68.2)	28 (62.2)	0.555
Maximum malapposition distance, mm	0.5±0.4	0.35±0.19	0.67±0.48	0.001
Malapposition >0.4 mm	26 (45.6)	9 (30.0)	17 (62.96)	0.013
Dissections				
Proximal edge dissection	9 (10.5)	4 (9.1)	5 (11.9)	0.670
Distal edge dissection	11 (12.8)	6 (13.64)	5 (11.9)	0.810

Data are presented as mean±SD or n (%). *Mean reference lumen area=(proximal reference lumen area+distal reference lumen area)/2. **Data are available for 90 lesions. $Mean reference lumen diameter=(proximal reference lumen diameter+distal reference lumen diameter)/2. #OCT calcium score based on the publication by Fujino et al[12]. IVL: intravascular lithotripsy; MLA: minimum lumen area; No.: number; OCT: optical coherence tomography

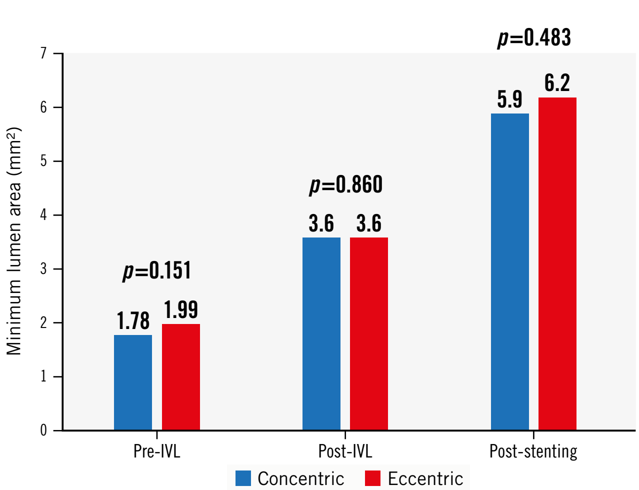

Figure 2. *Changes in minimum lumen area by optical coherence tomography (OCT) from baseline to after IVL, and after stenting. IVL: intravascular lithotripsy*

(15.4%). Ali et al have also previously examined the effect of IVL on calcified nodules[9]. In their study, the rate of fracture within a nodule itself was not reported; however, the rate of fracture within a lesion containing a nodule was 78.9%, in line with our study[9]. This finding is unsurprising given that the lesions containing nodules were severely calcified, with a mean calcium arc of 170 degrees. However, despite less fracture, a sequential increase in MLA and a large subsequent MSA at the nodule site were noted, with stent expansion at this site being >100%. This was despite most nodules remaining non-deformed with residual luminal protrusion following stenting. This finding suggests that there is perhaps a different mechanism explaining the stent expansion seen at the nodule site. Greater dissection at this site, as seen by OCT in our study, may be a possible explanation. Additionally, the presence of microfracture, which is beyond the resolution of OCT, may be another explanation, but likely requires histological studies to further examine this hypothesis. Regardless of the mechanism, and despite stent expansion of >100%, significant malapposition was common at the nodule site. Further studies are required to determine if the use of combination calcium

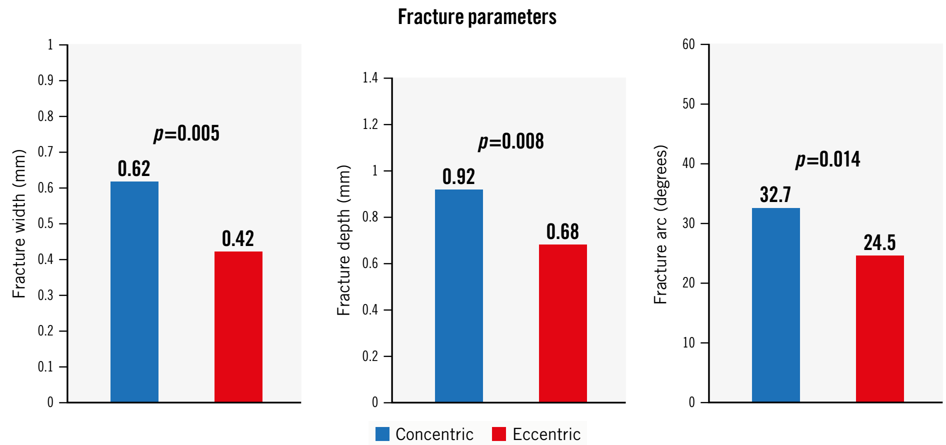

Figure 3. *Fracture parameters in concentric and eccentric lesions including fracture width, fracture depth and fracture arc.*

Table 5. Optical coherence tomography assessment of lesions containing a calcified nodule pre-IVL, post-IVL, and post-stenting.

OCT parameters	N=28
Vessel with nodule	
Left main	2 (7.14)
LAD	13 (46.4)
LCx	4 (14.3)
RCA	9 (32.1)
Baseline OCT assessment pre-IVL	
Baseline calcified nodule lesion assessment	
Maximum calcium arc in CN lesion, degrees	282.16±69.74
Mean calcium arc in CN lesion, degrees	170.36±57.00
Maximum calcium thickness, mm	1.27±0.24
Calcium volume index	3,477±2,279
Baseline nodule assessment	
Nodule morphology	
Eruptive nodule	11 (39.3)
Non-eruptive nodule	16 (57.0)
Nodule arc, degrees	109.2±34
Nodule protrusion into the lumen, mm	0.86±0.43
Nodule length, mm	4.6±2.8
Lumen area at nodule, mm^2	3.2±1.5
Percentage area stenosis at nodule, %	44.7±35.4
Assessment post-IVL	
Area at nodule site, mm^2	4.89±1.60
Dissection at nodule site	15 (57.69)
Fracture at nodule site	4 (15.38)
Fracture within lesion containing a nodule	19 (70.4)
Percentage area stenosis at nodule, %	23.94±26.17
Assessment post-stenting	
Deformation	11 (40.7)
Area at nodule site, mm^2	7.7±1.65
Percentage expansion at nodule site, %	103.6±27.2
Expansion <80% at nodule site	6 (23)
Malapposition at nodule site	14 (58.3)
Malapposition along length of lesion containing a nodule	21 (77.8)
Maximum malapposition distance, mm	0.548±0.41
Malapposition >0.4 mm	20 (71.4)

Data are presented as n (%) or mean±SD. CN: calcified nodule; IVL: intravascular lithotripsy; LAD: left anterior descending artery; LCx: left circumflex artery; OCT: optical coherence tomography; RCA: right coronary artery; SD: standard deviation

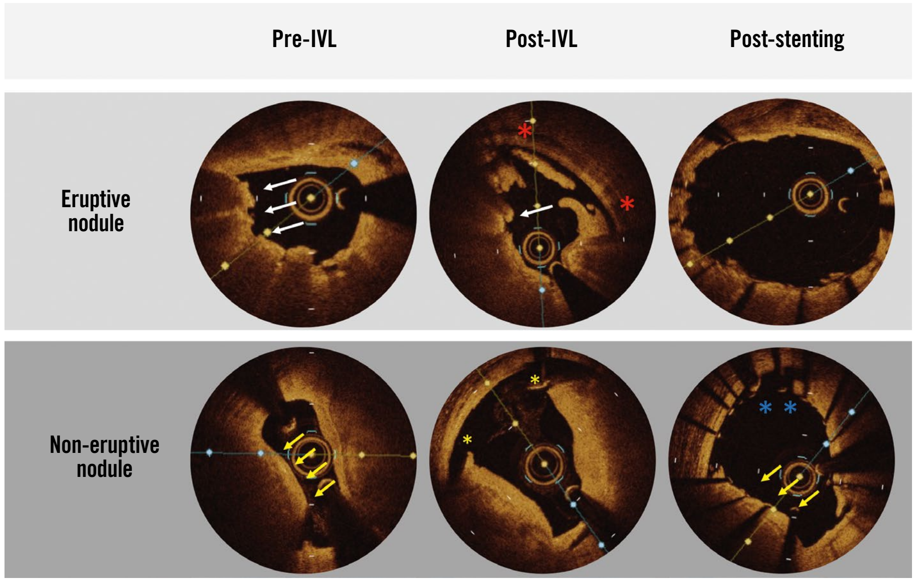

Figure 4. *Typical optical coherence tomography findings of an eruptive and non-eruptive nodule. Note the irregular protrusion of the eruptive nodule into the lumen with a thin fibrous cap (white arrows). Conversely, the non-eruptive nodule demonstrates a thick fibrous cap (yellow arrows). After IVL, significant disruption can be seen at the nodule site in both the eruptive and non-eruptive nodules with dissection (red and yellow asterisks); however, fracture is not seen. After stenting, the eruptive nodule is deformed and no longer protrudes into the lumen, while the non-eruptive nodule is not deformed and continues to protrude (yellow arrows). The presence of malapposition can also be seen in the non-deformed nodule (blue asterisks). IVL: intravascular lithotripsy*

modification therapies could lead to greater nodule deformation with reduced malapposition following stenting.

The safety of IVL is once again confirmed in our study. Intraprocedural complications were low overall, with perforation and slow flow/no reflow being uncommon. Despite dissection being seen on OCT in up to 75% of patients, flow-limiting dissection was rare. Intraprocedural complications, particularly perforation, have heretofore been a considerable drawback when using advanced calcium modification techniques. In studies using rotational atherectomy, perforation rates have been in the region of 2-4%[14,15], while modified balloons and super-high pressure balloons have demonstrated similar rates[18,19]. The improved safety profile with IVL is likely related to both the mechanism of action, which does not generate particulate matter that causes distal embolisation and slow/no flow, and the familiarity/ease of use for most interventional cardiologists of this balloon-based technology which uses low inflation pressures. Other registries and comparisons of IVL to other calcium modification technologies are ongoing (ClinicalTrials.gov: NCT04253171, NCT04428177, NCT04181268, NCT04298307).

The midterm outcomes in our cohort were akin to those seen in the 1-year follow-up of the Disrupt CAD III study[32]. Overall TLR and cardiac death rates were low and lower than those seen in previous studies of patients with severely calcified lesions undergoing PCI. A pooled analysis of the HORIZONS-AMI and ACUITY trials demonstrated a cardiac death rate of 4.0% and TLR rate of 8.7% at 1 year in patients with severely calcified lesions[1]. While the lower events rates in our study may be partially attributed to our smaller sample size, the mandatory use of intracoronary imaging before IVL, after IVL, and after stenting, which has been shown to reduce TLR rates, may have played a significant role[2,4,33-35].

Limitations

A number of limitations must be acknowledged. Firstly, this is a single-arm trial without any comparison between IVL and other calcium modification tools. Secondly, predilation was allowed in the protocol if an OCT catheter could not be advanced, and, while atherectomy techniques were not permitted, cutting/scoring balloons were allowed; these were subsequently used in ~22% of lesions before IVL and ~22% after IVL. This may have led to dissections and calcium fracture that were attributed to IVL treatment. Thirdly, a number of lesions were excluded from analysis due to poor OCT pullback quality, although this number was small (7 lesions). Newer software, such as Ultreon (Abbott), that incorporates the use of artificial intelligence to detect calcium may reduce the number of OCT pullbacks deemed unsuitable for analysis. A number of parameters had numerically but not statistically significant differences, and this lack of statistical significance may have been due to the small sample size.

Conclusions

In this prospective, multicentre study, IVL was both safe and effective in different calcium morphologies, with no differences found in MSA or stent expansion between concentric and eccentric calcium despite a greater number of visible fractures in concentric calcification.

Authors' affiliations

1. Department of Interventional Cardiology, Hospital Clínico San Carlos, IdISSC, Universidad Complutense de Madrid, Madrid, Spain; 2. Department of Cardiology, Hospital Universitario La Princesa, IIS-IP, CIBER-CV, Madrid, Spain; 3. Interventional Cardiology Unit, San Luigi Gonzaga University Hospital, Orbassano, Italy; 4. Rivoli Infermi Hospital, Rivoli, Turin, Italy; 5. Department of Cardiology, Hospital Universitario Virgen de la Arrixaca, Murcia, Spain; 6. Department of Cardiology, Hospital Universitario de León, León, Spain; 7 Cardiology Department, Hospital Clínic Cardiovascular Institute, Hospital Clínic Barcelona, Institut d'Investigacions Biomèdiques August Pi i Sunyer, Barcelona, Spain; 8. Departamento de Cardiología Intervencionista, Hospital del Mar, IMIM, Universidad Autónoma, Barcelona, Spain; 9. Departamento de Cardiología Intervencionista, Servicio de Cardiología, Hospital Universitario la Paz, Madrid, Spain; 10. Cardiac Department, Hospital Santa Creu i Sant Pau, Barcelona, Spain; 11. Hospital Universitario Marques de Valdecilla, IDIVAL, Santander, Spain; 12. CIBERCV, Instituto de Ciencias del Corazón (ICICOR), Hospital Clínico Universitario de Valladolid, Valladolid, Spain; 13. Interventional Cardiology, Hospital Álvaro Cunqueiro, Vigo, Spain

Acknowledgements

The authors would like to thank Josep Gomez Lara from the Hospital Universitari de Bellvitge for his guidance on reviewing the manuscript.

Guest Editor

This paper was guest edited by Franz-Josef Neumann, MD, PhD, FESC; *Department of Cardiology and Angiology II, University Heart Center Freiburg - Bad Krozingen, Bad Krozingen, Germany.*

Funding

This study was supported by an unrestricted grant from Abbott.

Conflict of interest statement

N. Gonzalo has received a research grant from Abbott; and consultancy and speaker fees from Abbott, Boston Scientific, Shockwave Medical, Abiomed, and Philips. A. McInerney has received speaker fees from Shockwave Medical, Boston Scientific, and Novartis. I. Amat Santos declares acting as a proctor for Boston Scientific. A. Pérez de Prado reports receiving institutional research grants from Abbott and Shockwave Medical. A. Jurado-Roman has received speaker fees from Shockwave Medical and Abbott. The other authors have no conflicts of interest to declare. The Guest Editor reports lecture fees paid to his institution from Amgen, Bayer HealthCare, Biotronik, Boehringer Ingelheim, Boston Scientific, Daiichi Sankyo, Edwards Lifesciences, Ferrer, Pfizer, and Novartis; consultancy fees paid to his institution from Boehringer Ingelheim; and grant support from Bayer HealthCare, Boston Scientific, Biotronik, Edwards Lifesciences, GlaxoSmithKline, Medtronic, and Pfizer.

References

1. Généreux P, Madhavan MV, Mintz GS, Maehara A, Palmerini T, Lasalle L, Xu K, McAndrew T, Kirtane A, Lansky AJ, Brener SJ, Mehran R, Stone GW. Ischemic outcomes after coronary intervention of calcified vessels in acute coronary syndromes. Pooled analysis from the HORIZONS-AMI (Harmonizing Outcomes With Revascularization and Stents in Acute Myocardial Infarction) and ACUITY (Acute Catheterization and Urgent Intervention Triage Strategy) TRIALS. *J Am Coll Cardiol.* 2014;63:1845-54.
2. Zhang J, Gao X, Kan J, Ge Z, Han L, Lu S, Tian N, Lin S, Lu Q, Wu X, Li Q, Liu Z, Chen Y, Qian X, Wang J, Chai D, Chen C, Li X, Gogas BD, Pan T, Shan S, Ye F, Chen SL. Intravascular Ultrasound Versus Angiography-Guided Drug-Eluting Stent Implantation: The ULTIMATE Trial. *J Am Coll Cardiol.* 2018;72:3126-37.
3. Kang SJ, Ahn JM, Song H, Kim WJ, Lee JY, Park DW, Yun SC, Lee SW, Kim YH, Lee CW, Mintz GS, Park SW, Park SJ. Comprehensive intravascular ultrasound assessment of stent area and its impact on restenosis and adverse cardiac events in 403 patients with unprotected left main disease. *Circ Cardiovasc Interv.* 2011;4:562-9.
4. Gao XF, Ge Z, Kong XQ, Kan J, Han L, Lu S, Tian NL, Lin S, Lu QH, Wang XY, Li QH, Liu ZZ, Chen Y, Qian XS, Wang J, Chai DY, Chen CH, Pan T, Ye F, Zhang JJ, Chen SL; ULTIMATE Investigators. 3-Year Outcomes of the ULTIMATE Trial Comparing Intravascular Ultrasound Versus Angiography-Guided Drug-Eluting Stent Implantation. *JACC Cardiovasc Interv.* 2021;14:247-57.
5. Alfonso F, Macaya C, Goicolea J, Hernandez R, Segovia J, Zamorano J, Bañuelos C, Zarco P. Determinants of coronary compliance in patients with coronary artery disease: an intravascular ultrasound study. *J Am Coll Cardiol.* 1994;23:879-84.
6. Kereiakes DJ, Virmani R, Hokama JY, Illindala U, Mena-Hurtado C, Holden A, Hill JM, Lyden SP, Ali ZA. Principles of Intravascular Lithotripsy for Calcific Plaque Modification. *JACC Cardiovasc Interv.* 2021;14:1275-92.
7. Blachutzik F, Honton B, Escaned J, Hill JM, Werner N, Banning AP, Lansky AJ, Schlattner S, De Bruyne B, Di Mario C, Dörr O, Hamm C, Nef HM. Safety and effectiveness of coronary intravascular lithotripsy in eccentric calcified coronary lesions: a patient-level pooled analysis from the Disrupt CAD I and CAD II Studies. *Clin Res Cardiol.* 2021;110:228-36.
8. Wang X, Matsumura M, Mintz GS, Lee T, Zhang W, Cao Y, Fujino A, Lin Y, Usui E, Kanaji Y, Murai T, Yonetsu T, Kakuta T, Maehara A. In Vivo Calcium Detection by Comparing Optical Coherence Tomography, Intravascular Ultrasound, and Angiography. *JACC Cardiovasc Imaging.* 2017;10:869-79.
9. Ali ZA, Kereiakes D, Hill J, Saito S, Di Mario C, Honton B, Gonzalo N, Riley R, Maehara A, Matsumura M, Stone GW, Shlofmitz R. Safety and Effectiveness of Coronary Intravascular Lithotripsy for Treatment of Calcified Nodules. *JACC Cardiovasc Interv.* 2023;16:1122-4.
10. Garcia-Garcia HM, McFadden EP, Farb A, Mehran R, Stone GW, Spertus J, Onuma Y, Morel MA, van Es GA, Zuckerman B, Fearon WF, Taggart D, Kappetein AP, Krucoff MW, Vranckx P, Windecker S, Cutlip D, Serruys PW; Academic Research Consortium. Standardized End Point Definitions for Coronary Intervention Trials: The Academic Research Consortium-2 Consensus Document. *Circulation.* 2018;137:2635-50.
11. Tearney GJ, Regar E, Akasaka T, Adriaenssens T, Barlis P, Bezerra HG, Bouma B, Bruining N, Cho JM, Chowdhary S, Costa MA, de Silva R, Dijkstra J, Di Mario C, Dudek D, Falk E, Feldman MD, Fitzgerald P, Garcia-Garcia HM, Gonzalo N, Granada JF, Guagliumi G, Holm NR, Honda Y, Ikeno F, Kawasaki M, Kochman J, Koltowski L, Kubo T, Kume T, Kyono H, Lam CC, Lamouche G, Lee DP, Leon MB, Maehara A, Manfrini O, Mintz GS, Mizuno K, Morel MA, Nadkarni S, Okura H, Otake H, Pietrasik A, Prati F, Räber L, Radu MD, Rieber J, Riga M, Rollins A, Rosenberg M, Sirbu V, Serruys PW, Shimada K, Shinke T, Shite J, Siegel E, Sonoda S, Suter M, Takarada S, Tanaka A, Terashima M, Thim T, Uemura S, Ughi GJ, van Beusekom HM, van der Steen AF, van Es GA, van Soest G, Virmani R, Waxman S, Weissman NJ, Weisz G; International Working Group for Intravascular Optical Coherence Tomography (IWG-IVOCT). Consensus standards for acquisition, measurement, and reporting of intravascular optical coherence tomography studies: a report from the International Working Group for Intravascular Optical Coherence Tomography Standardization and Validation. *J Am Coll Cardiol.* 2012;59:1058-72.
12. Fujino A, Mintz GS, Matsumura M, Lee T, Kim SY, Hoshino M, Usui E, Yonetsu T, Haag ES, Shlofmitz RA, Kakuta T, Maehara A. A new optical

coherence tomography-based calcium scoring system to predict stent underexpansion. *EuroIntervention.* 2018;13:e2182-9.

13. Suwannasom P, Sotomi Y, Asano T, Koon JN, Tateishi H, Zeng Y, Tenekecioglu E, Wykrzykowska JJ, Foin N, de Winter RJ, Ormiston JA, Serruys PW, Onuma Y. Change in lumen eccentricity and asymmetry after treatment with Absorb bioresorbable vascular scaffolds in the ABSORB cohort B trial: a five-year serial optical coherence tomography imaging study. *EuroIntervention.* 2017;12:e2244-52.

14. Abdel-Wahab M, Richardt G, Joachim Büttner H, Toelg R, Geist V, Meinertz T, Schofer J, King L, Neumann FJ, Khattab AA. High-speed rotational atherectomy before paclitaxel-eluting stent implantation in complex calcified coronary lesions: the randomized ROTAXUS (Rotational Atherectomy Prior to Taxus Stent Treatment for Complex Native Coronary Artery Disease) trial. *JACC Cardiovasc Interv.* 2013;6:10-9.

15. Abdel-Wahab M, Toelg R, Byrne RA, Geist V, El-Mawardy M, Allali A, Rheude T, Robinson DR, Abdelghani M, Sulimov DS, Kastrati A, Richardt G. High-Speed Rotational Atherectomy Versus Modified Balloons Prior to Drug-Eluting Stent Implantation in Severely Calcified Coronary Lesions. *Circ Cardiovasc Interv.* 2018;11:e007415.

16. Parikh K, Chandra P, Choksi N, Khanna P, Chambers J. Safety and feasibility of orbital atherectomy for the treatment of calcified coronary lesions: the ORBIT I trial. *Catheter Cardiovasc Interv.* 2013;81:1134-9.

17. Chambers JW, Feldman RL, Himmelstein SI, Bhatheja R, Villa AE, Strickman NE, Shlofmitz RA, Dulas DD, Arab D, Khanna PK, Lee AC, Ghali MG, Shah RR, Davis TP, Kim CY, Tai Z, Patel KC, Puma JA, Makam P, Bertolet BD, Nseir GY. Pivotal trial to evaluate the safety and efficacy of the orbital atherectomy system in treating de novo, severely calcified coronary lesions (ORBIT II). *JACC Cardiovasc Interv.* 2014;7:510-8.

18. Rheude T, Rai H, Richardt G, Allali A, Abdel-Wahab M, Sulimov DS, Mashayekhi K, Ayoub M, Cuculi F, Bossard M, Kufner S, Xhepa E, Kastrati A, Fusaro M, Joner M, Byrne RA, Cassese S. Super high-pressure balloon versus scoring balloon to prepare severely calcified coronary lesions: the ISAR-CALC randomised trial. *EuroIntervention.* 2021;17:481-8.

19. Mangieri A, Nerla R, Castriota F, Reimers B, Regazzoli D, Leone PP, Gasparini GL, Khokhar AA, Laricchia A, Giannini F, Casale F, Bezzeccheri A, Briguori C, Colombo A. Cutting balloon to optimize predilation for stent implantation: The COPS randomized trial. *Catheter Cardiovasc Interv.* 2023;101:798-805.

20. Kereiakes DJ, Di Mario C, Riley RF, Fajadet J, Shlofmitz RA, Saito S, Ali ZA, Klein AJ, Price MJ, Hill JM, Stone GW. Intravascular Lithotripsy for Treatment of Calcified Coronary Lesions: Patient-Level Pooled Analysis of the Disrupt CAD Studies. *JACC Cardiovasc Interv.* 2021;14:1337-48.

21. Mody R, Dash D, Mody B, Maligireddy AR, Agrawal A, Rastogi L, Monga IS. Can Most Calcified Coronary Stenosis Be Optimized With Coronary Intravascular Lithotripsy? *JACC Asia.* 2023;3:185-97.

22. Mattesini A, Nardi G, Martellini A, Sorini Dini C, Hamiti B, Stolcova M, Meucci F, Di Mario C. Intravascular Imaging to Guide Lithotripsy in Concentric and Eccentric Calcific Coronary Lesions. *Cardiovasc Revasc Med.* 2020;21:1099-105.

23. Emori H, Shiono Y, Kuriyama N, Honda Y, Ebihara S, Kadooka K, Ogata K, Kimura T, Nishihira K, Tanaka A, Shibata Y. Calcium Fracture After Intravascular Lithotripsy as Assessed With Optical Coherence Tomography. *Circ J.* 2023;87:799-805.

24. Pinilla-Echeverri N, Bossard M, Hillani A, Chavarria JA, Cioffi GM, Dutra G, Guerrero F, Madanchi M, Attinger A, Kossmann E, Sibbald M, Cuculi F, Sheth T. Treatment of Calcified Lesions Using a Dedicated Super-High Pressure Balloon: Multicenter Optical Coherence Tomography Registry. *Cardiovasc Revasc Med.* 2023;52:49-58.

25. Hemetsberger R, Gori T, Toelg R, Byrne R, Allali A, El-Mawardy M, Rheude T, Weissner M, Sulimov DS, Robinson DR, Richardt G, Abdel-Wahab M. Optical Coherence Tomography Assessment in Patients Treated With Rotational Atherectomy Versus Modified Balloons: PREPARE-CALC OCT. *Circ Cardiovasc Interv.* 2021;14:e009819.

26. Ali ZA, Nef H, Escaned J, Werner N, Banning AP, Hill JM, De Bruyne B, Montorfano M, Lefevre T, Stone GW, Crowley A, Matsumura M, Maehara A, Lansky AJ, Fajadet J, Di Mario C. Safety and Effectiveness of Coronary Intravascular Lithotripsy for Treatment of Severely Calcified Coronary Stenoses: The Disrupt CAD II Study. *Circ Cardiovasc Interv.* 2019;12:e008434.

27. Hill JM, Kereiakes DJ, Shlofmitz RA, Klein AJ, Riley RF, Price MJ, Herrmann HC, Bachinsky W, Waksman R, Stone GW; Disrupt CAD III Investigators. Intravascular Lithotripsy for Treatment of Severely Calcified Coronary Artery Disease. *J Am Coll Cardiol.* 2020;76:2635-46.

28. Amemiya K, Maehara A, Yamamoto MH, Oyama Y, Igawa W, Ono M, Kido T, Ebara S, Okabe T, Yamashita K, Isomura N, Mintz GS, Ochiai M. Chronic stent recoil in severely calcified coronary artery lesions. A serial optical coherence tomography study. *Int J Cardiovasc Imaging.* 2020;36:1617-26.

29. Pengchata P, Pongakasira R, Wongsawangkit N, Phichaphop A, Wongpraparut N. Characteristics and Pattern of Calcified Nodule and/or Nodular Calcification Detected by Intravascular Ultrasound on the Device-Oriented Composite Endpoint (DoCE) in Patients with Heavily Calcified Lesions Who Underwent Rotational Atherectomy-Assisted Percutaneous Coronary Intervention. *J Interv Cardiol.* 2023;2023:6456695.

30. Lee T, Mintz GS, Matsumura M, Zhang W, Cao Y, Usui E, Kanaji Y, Murai T, Yonetsu T, Kakuta T, Maehara A. Prevalence, Predictors, and Clinical Presentation of a Calcified Nodule as Assessed by Optical Coherence Tomography. *JACC Cardiovasc Imaging.* 2017;10:883-91.

31. Torii S, Sato Y, Otsuka F, Kolodgie FD, Jinnouchi H, Sakamoto A, Park J, Yahagi K, Sakakura K, Cornelissen A, Kawakami R, Mori M, Kawai K, Amoa F, Guo L, Kutyna M, Fernandez R, Romero ME, Fowler D, Finn AV, Virmani R. Eruptive Calcified Nodules as a Potential Mechanism of Acute Coronary Thrombosis and Sudden Death. *J Am Coll Cardiol.* 2021;77:1599-611.

32. Kereiakes DJ, Hill JM, Shlofmitz RA, Klein AJ, Riley RF, Price MJ, Herrmann HC, Bachinsky W, Waksman R, Stone GW; Disrupt CAD III Investigators. Intravascular Lithotripsy for Treatment of Severely Calcified Coronary Lesions: 1-Year Results From the Disrupt CAD III Study. *J Soc Cardiovasc Angiogr Interv*. 2022;1:100001.

33. Hong SJ, Kim BK, Shin DH, Nam CM, Kim JS, Ko YG, Choi D, Kang TS, Kang WC, Her AY, Kim YH, Hur SH, Hong BK, Kwon H, Jang Y, Hong MK; IVUS-XPL Investigators. Effect of Intravascular Ultrasound-Guided vs Angiography-Guided Everolimus-Eluting Stent Implantation: The IVUS-XPL Randomized Clinical Trial. *JAMA.* 2015;314:2155-63.

34. Hong SJ, Mintz GS, Ahn CM, Kim JS, Kim BK, Ko YG, Kang TS, Kang WC, Kim YH, Hur SH, Hong BK, Choi D, Kwon H, Jang Y, Hong MK; IVUS-XPL Investigators. Effect of Intravascular Ultrasound-Guided Drug-Eluting Stent Implantation: 5-Year Follow-Up of the IVUS-XPL Randomized Trial. *JACC Cardiovasc Interv.* 2020;13:62-71.

35. Lee JM, Choi KH, Song YB, Lee JY, Lee SJ, Lee SY, Kim SM, Yun KH, Cho JY, Kim CJ, Ahn HS, Nam CW, Yoon HJ, Park YH, Lee WS, Jeong JO, Song PS, Doh JH, Jo SH, Yoon CH, Kang MG, Koh JS, Lee KY, Lim YH, Cho YH, Cho JM, Jang WJ, Chun KJ, Hong D, Park TK, Yang JH, Choi SH, Gwon HC, Hahn JY; RENOVATE-COMPLEX-PCI Investigators. Intravascular Imaging-Guided or Angiography-Guided Complex PCI. *N Engl J Med.* 2023;388:1668-79.

Supplementary data

Supplementary Figure 1. The number of patients enrolled and finally included in the study. Final groupings of calcium morphology as defined using optical coherence tomography.

Supplementary Figure 2. Freedom from all-cause mortality at 12 months following IVL therapy for calcified coronary artery disease.

Supplementary Figure 3. Freedom from target lesion revascularisation at 12 months following IVL therapy for calcified coronary artery disease.

The supplementary data are published online at: https://eurointervention.pcronline.com/doi/10.4244/EIJ-D-23-00605

Supplementary data

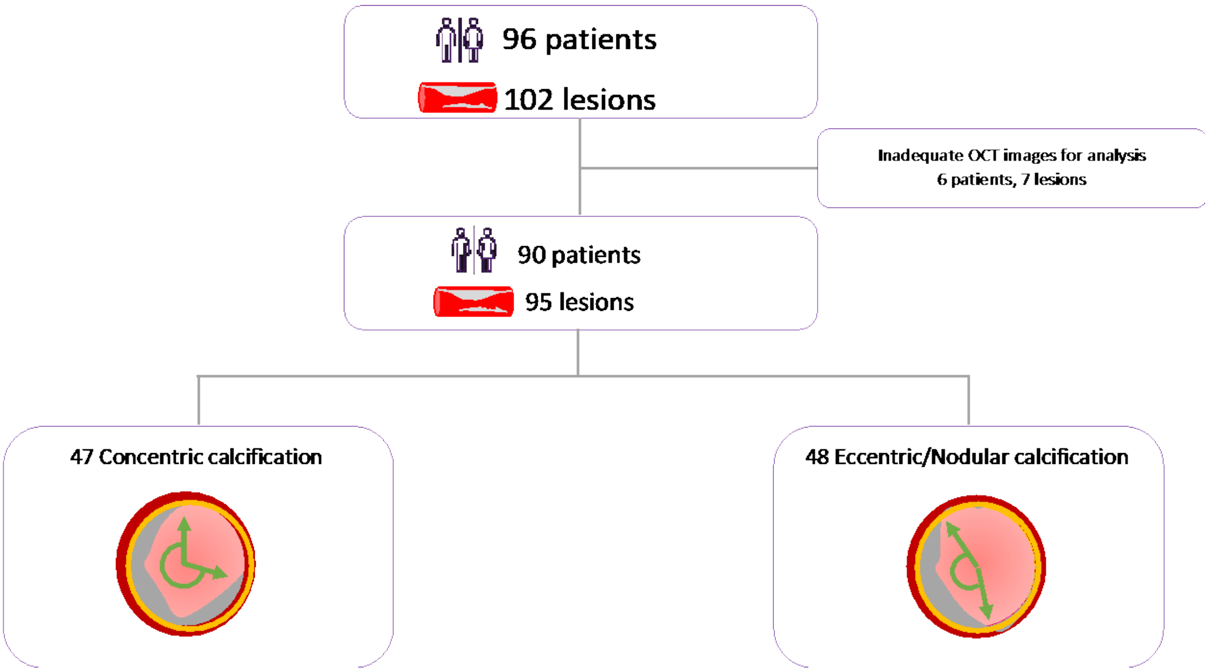

Supplementary Figure 1. The number of patients enrolled, and finally included in the study. Final groupings of calcium morphology as defined using optical coherence tomography.

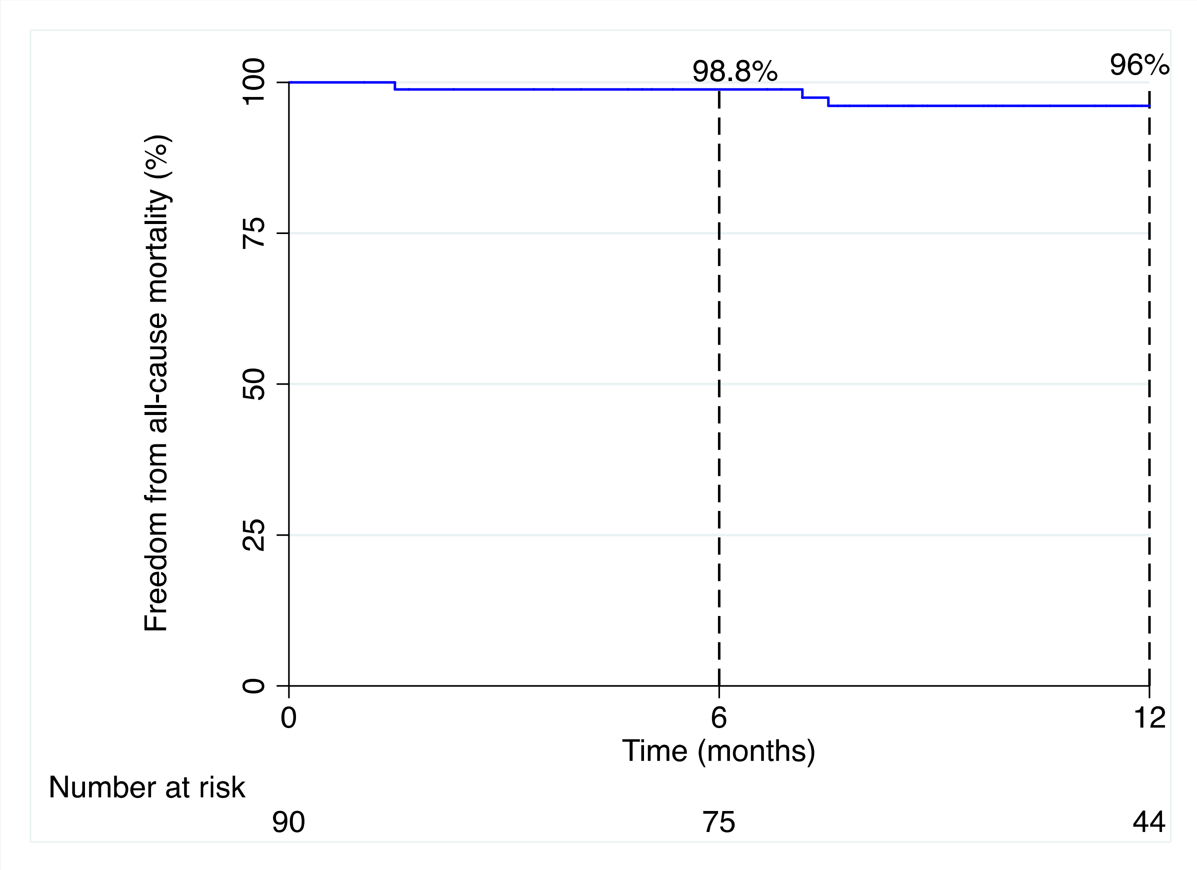

Supplementary Figure 2. Freedom from all-cause mortality at 12 months following IVL therapy for calcified coronary artery disease.

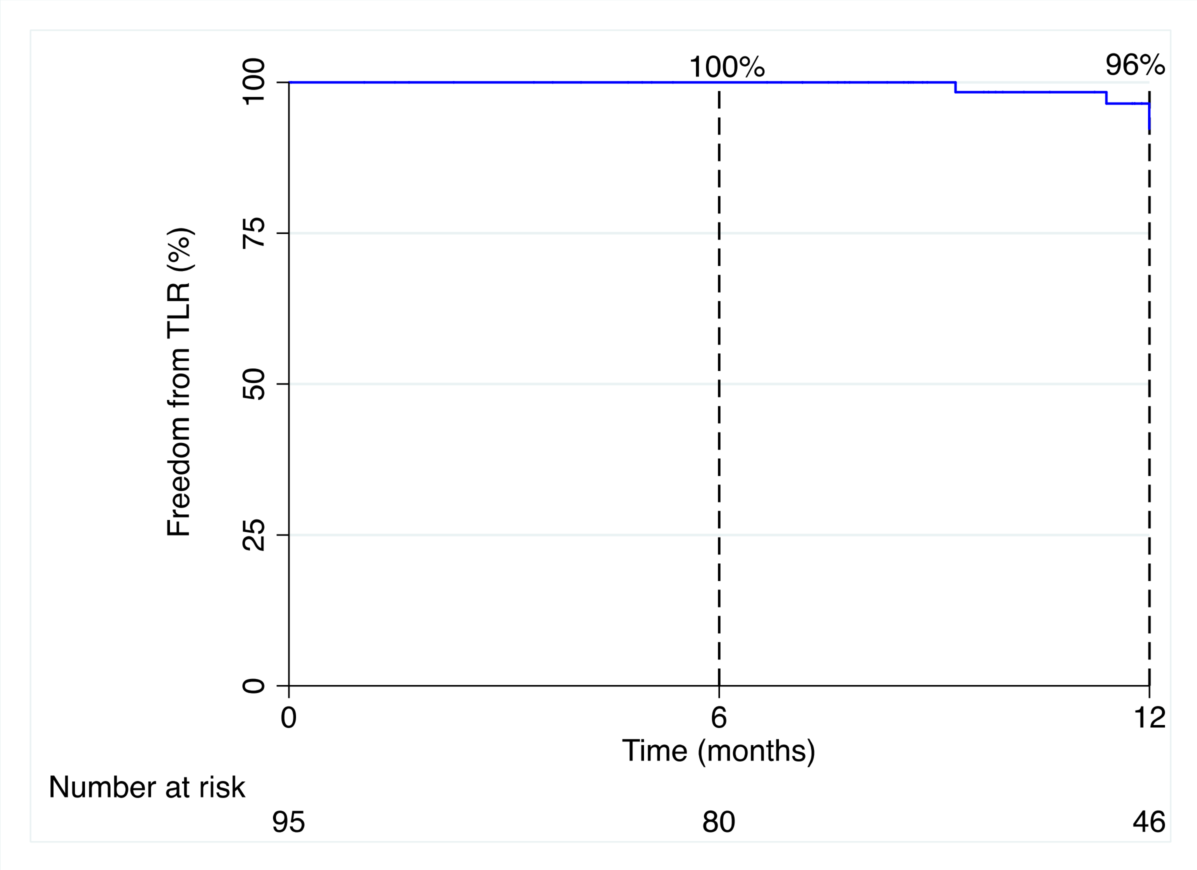

Supplementary Figure 3. Freedom from target lesion revascularisation at 12 months following IVL therapy for calcified coronary artery disease.